Center of mass quantization of excitons in $Zn_{1-x}Cd_xSe/ZnSe$ quantum-wells

D. Greco and R. Cingolani
Unita Istituto Nazionale della Fisica Materia, Dipartimento di Scienza dei Materiali, Università di Lecce, Via Arnesano, I-73100 Lecce, Italy

A. D'Andrea and N. Tommasini
Istituto di Metodologie Avanzate Inorganiche, CNR Area della Ricerca di Roma, Montelibretti, Italy

L. Vanzetti* and A. Franciosi†
Laboratorio Tecnologie Avanzate Superfici e Catalisi, Istituto Nazionale di Fisica della Materia, Area di Ricerca, Padriciano 99, Trieste, Italy
(Received 2 November 1995)

Absorption and photoluminescence studies of $Zn_{1-x}Cd_xSe/ZnSe$ quantum wells, with well thicknesses at the crossover between two- and three-dimensional exciton behaviors, show clear evidence of quantization of the exciton-polariton center-of-mass motion. A thin-slab variational wave function model is used to reproduce the energy and the dispersion of the center-of-mass states. [S0163-1829(96)06131-0]

I. INTRODUCTION

An increasing number of spectroscopic studies is focusing on the optical properties of excitons in $Zn_{1-x}Cd_xSe/ZnSe$ quantum wells (QW's), since the first demonstration of blue-green lasers based on such structures.[1,2] Excitons in these materials are found to play an important role in determining the properties relevant to optoelectronic devices, such as lasing and nonlinear absorption, because of the large exciton screening threshold and strong thermal stability even at room temperature.[3–5]

In this paper, we report evidence of quantization of the exciton-polariton center-of-mass (CM) motion in $Zn_{1-x}Cd_xSe/ZnSe$ QW's. This study has a twofold interest. First, evidence of quantization of CM motion has been previously reported in binary *III-V* (Refs. 6,7) and *II-VI* QW's,[8–11] but, to our knowledge, has never been observed in ternary alloy QW's. Indeed, center-of-mass quantization is widely considered as an indication of high crystalline perfection and homogeneity within the QW's, with a substantial polariton character of the free exciton. Second,the investigated $Zn_{1-x}Cd_xSe/ZnSe$ heterostructures have a well thickness covering the intermediate region between two- and three-dimensional exciton behaviors, allowing a precise study of the excitonic properties as a function of the quantization potential.

We measured the photoluminescence (PL) and absorption spectra in quantum wells with well width values ranging from 2.5 to 5 times the exciton Bohr radius a_B. The quantum wells excitons are described within the effective-mass approximation using a variational envelope function.[8,9] This model is able to reproduce the energy positions of the exciton resonances in the absorption spectra, providing the well width dependence of the CM states up to $n=3$. The variational treatment employed in this work provides the quantized values of the exciton-polariton wave vector within the $Zn_{1-x}Cd_xSe/ZnSe$ QW's. This allows an independent confirmation of our explanation, by comparing the $E(k)$ dispersion of the quantized states with the theoretical polariton curve.

II. EXPERIMENT

The samples examined were grown by solid source molecular beam epitaxy on GaAs (001) substrates, in the form of ten QW periods consisting of $Zn_{0.89}Cd_{0.11}Se/ZnSe$. After thermal removal of the native GaAs oxide, a 0.5-μm *n*-GaAs buffer layer was grown at 580 °C. The sample was then cooled under As flux and prepared for the deposition at 290 °C of 1.5-μm ZnSe buffer layer to relax the lattice mismatch with the GaAs. The multiple quantum well (MQW) was then fabricated at 250 °C with a growth interruption of 30 sec at each interface. Details on the metodology employed can be found elsewhere.[13,14]

In this work, we concentrate on three samples having well width values of 7 nm ($L_w=2.5a_B$), 11 nm ($L_w=3.4a_B$), and 20 nm ($L_w=5a_B$), and a constant ZnSe barrier width of 20 nm. The large barrier thickness results in decoupled quantum wells in the whole structure. With such structural parameters, the MQW's are grown pseudomorfically on the ZnSe buffer layer, with a substantial compressive strain within the quantum wells that reflects the large in-plane lattice mismatch (0.7%) of the $Zn_{0.89}Cd_{0.11}Se$ alloy relative to the binary buffer.

For transmission measurements, the heterostructures were processed as described in Ref. 4 to selectively remove the GaAs substrate. Absorption spectra from the remaining self-supporting films, comprised of the $Zn_{0.89}Cd_{0.11}Se$ MQW and the ZnSe buffer, were obtained by focusing light through the windows opened within the *III-V* substrate. Optical absorption and photoluminescence (PL) measurements were performed by mounting the samples on the cold finger of a closed-cycle He cryostat, operating in the range 10 K – 300 K. The PL measurements were performed through resonant excitation in the QW region, using the 4579.36 Å line of an Ar^+ laser in backscattering configuration and 5 mW of

 © 1996 The American Physical Society

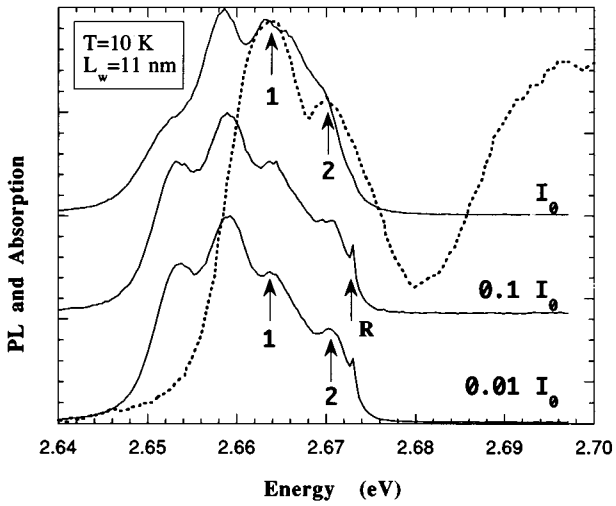

FIG. 1. Comparison between photoluminescence spectra (solid line) and optical absorption (dotted line) from ten periods $Zn_{1-x}Cd_xSe/ZnSe$ multiple quantum wells (MQW's) with $L_w = 11$ nm. PL spectra displaced upward correspond to increasing excitation intensities ($I_0 = 5$ mW on the sample). Luminescence signals in the low-energy tail of the free-exciton absorption resonance are extrinsic in nature, as demonstrated by the saturation under high excitation intensity. The Raman line (R) of the laser is also present. Numbers label the quantized center-of-mass states of the heavy hole exciton polariton.

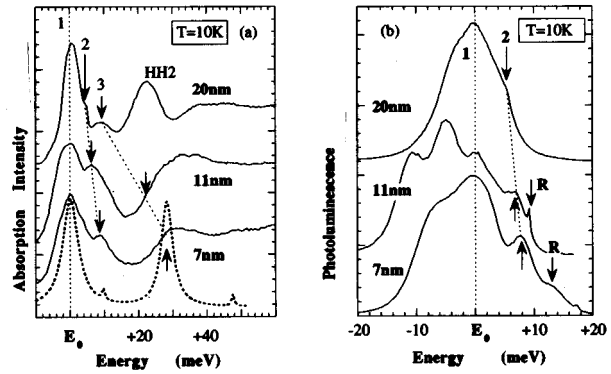

FIG. 2. Absorption (a) and luminescence (b) spectra from different $Zn_{1-x}Cd_xSe/ZnSe$ MQW's rigidly shifted to align the free-exciton spectral features. The vertical dotted line denotes the HH $n=1$ center-of-mass eigenstate, while vertical arrows indicate the $n=2$ and $n=3$ states. The calculated normal-incidence absorption spectrum of the 7-nm-wide well sample is also shown for comparison [dashed line in (a)]. The spectrum was computed using the variational wave functions of Eq. (4). Inhomogeneous broadening was taken on the order of 1 meV, while the absorption continuum was neglected in the calculations.

maximum power on the sample. The emission spectra were detected with a 0.85-m double monochromator and a cooled GaAs photon counter. Optical absorption spectra were obtained using the mechanically chopped light of a tungsten halogen lamp, the same monochromator and detector used in the PL measurements. The overall spectral resolution of the measurements was always better than 0.2-meV.

III. RESULTS AND DISCUSSION

In Fig. 1, we show the PL spectra (solid line) from the 11-nm-wide quantum wells recorded at a temperature of 10 K and for increasing excitation intensity. For comparison, we also show the absorption spectrum from the same sample (dashed line). The intensity dependence of the PL spectra exhibits a saturation of the two low-energy features at 2.653 and 2.659 eV, indicating the extrinsic nature of these transitions. This is confirmed by the absence of corresponding features in the absorption spectrum, which is expected to reflect more closely the intrinsic joint density of states of the QW's. The quantized states of CM motion of the exciton, are marked by vertical arrows and labeled by 1 and 2 in the PL spectra of Fig. 1. These features have a direct counterpart in the optical absorption spectrum, spanning over about 10 meV, which is less than the LO-phonon energy (31 meV) in the ternary alloy constituting the well. Under this condition, the fast LO-phonon-assisted relaxation into the lowest level is forbidden. The main remaining relaxation mechanisms are radiative electron-hole recombination and nonradiative recombination via longitudinal acoustical (LA) phonons. Due to the typical lifetime of these channels, on the order of 100 ps for e-h recombination and 1 μsec for LA-phonon relaxation, the radiative recombination is the most favorable and allows the observation of all excited levels. We should mention that the discrete spectral features 1 and 2 in Fig. 1 cannot be ascribed to well width fluctuations, as the expected monolayer splitting is about 1 meV at this well width. In the same way, they cannot be attributed to $2s$, $2p$, . . . exciton states or to the light hole exciton, because of the much larger energy splitting expected. Figures 2(a) and 2(b) show the existence of these high-energy resonances at various well widths, both in absorption and luminescence. The spectra have been rigidly shifted in order to align the heavy hole (HH) $n=1$ feature, diagonal dashed lines through the data and arrows indicate the experimental position of the states varying the well thickness. There is a good overall consistency between the energy positions of the center-of-mass states observed in the absorption and luminescence spectra. The energy splitting between CM states is found to decrease with the well width. Similar experiments on $Zn_{1-x}Cd_xSe/ZnSe$ QW's with 23% of cadmium content did not show any CM state, due to the strong spectral broadening caused by compositional fluctuations.

In what follows, we present a quantitative analysis of our experiments. The theory of excitons in thin layers distinguishes two regimes for the exciton behaviors, according to the relative values of the well width L_w and the exciton Bohr radius a_B. When L_w is smaller than the transverse extent of the exciton wave function ($L_w \leqslant 2a_B$), quantum confinement primarily affects the individual electron and hole wave functions. This is the so-called *strong confinement regime* (two-dimensional regime) in which the confinement energy of carriers $\hbar^2/mL_w^2$ is larger than the exciton binding energy.

In thicker wells (so-called *thin-film regime* with $L_w > 2a_B$) quantum confinement affects the exciton envelope function, whereas negligible effects are expected on individual carriers. In this case, the center-of-mass motion of the exciton becomes quantized,[8–10] resulting in a quantized exciton momentum ($\hbar k$) along the growth direction. This is the regime that we expect to recover in the MQW's investi-

gated ($2.5a_B < L_w < 5a_B$). To get a quantitative explanation of our experimental spectra, we have to consider the coupling between the exciton and the radiation field giving rise to the exciton polariton[15] in the well. The fundamental equation of the exciton-photon interaction, which gives rise to the polariton dispersion curves $E(k)$, is obtained by the semiclassical theory of nonlocal response by equating the photon dispersion law to the dielectric function with spatial dispersion:[16]

$$\varepsilon_\infty + \frac{4\pi\alpha_0 E_0^2}{E_0^2 - E^2 + \beta k^2 + i\gamma E} = \frac{\hbar^2 c^2}{E^2} k^2, \tag{1}$$

where ε_∞ is the dielectric constant, $4\pi\alpha_0$ is the oscillator strength, E_0 is the free exciton energy, $\beta = \hbar^2 E_0 / M_{\rm exc}$ with $M_{\rm exc}$ the total effective exciton mass, γ is the exciton broadening, k is the polariton wave vector. When the polariton is excitonlike with wavelength $\lambda_{\rm pol}$ and the potential well is infinite, the interference condition which originates standing waves corresponds to the quantization condition,

$$k_n = n\frac{\pi}{L_{\rm eff}}, \quad n = 1,2,3, \ldots \tag{2}$$

for the center-of-mass wave vector, where $L_{\rm eff}$ represents the quantization length of the exciton motion and corresponds to the extension over which the exciton wave function is appreciably different from zero.[12] The continuous polariton curve $E(k)$ transforms into a series of discrete points. In the excitonlike branch, the polariton curve can be approximately expressed by the exciton dispersion,

$$E_n^{\rm exc} = E_0 + \frac{\hbar^2}{2M_{\rm exc}}\left(\frac{\pi}{L_{\rm eff}}\right)^2 n^2. \tag{3}$$

This simple model strictly holds for large well widths and in the adiabatic approximation ($L_w > 10\,a_B$), when the center-of-mass and the *e*-*h* relative motions are decoupled. In our case ($2.5a_B < L_w < 5a_B$), this model can only give a qualitative description of the behaviors of the quantized states in the optical spectra (namely, the well width dependence of the energy splitting between peaks), because the quantization length $L_{\rm eff}$ is comparable to the depth over which an effective coupling of the CM and *e*-*h* relative motions takes place, namely, the ''*transition layer*.'' In order to reproduce the experimental quantization effects, we have to resort to a more refined ''*thin-slab*'' model, in which the quantum wells excitons can be described within the effective mass approximation by the variational envelope functions,[9] including nonadiabatic terms,

$$\begin{aligned}\Psi_K^e(r,Z) &= N^e[\cos(KZ) - F_{\rm ee}(z)\cosh(PZ) \\ &\quad + F_{\rm eo}(z)\sinh(PZ)]\exp(-r/a_B), \\ \Psi_K^o(r,Z) &= N^o[\sin(KZ) + F_{\rm oe}(z)\sinh(PZ) \\ &\quad - F_{\rm oo}(z)\cosh(PZ)]\exp(-r/a_B),\end{aligned} \tag{4}$$

for even (e) and odd (o) parity, respectively. It has been shown[8,9] that this description is valid for quantum wells wider than $2.5a_B$. In Eq. (4), we assume that the exciton is perfectly confined in a one-dimensional well, N^e and N° are normalization coefficients, K represents the CM wave vector of the excitons, $Z = z_e m_e / M_{\rm exc} + z_h m_h / M_{\rm exc}$ is the exciton center-of-mass position along the z axis, $1/P$ is the variational parameter which corresponds to the depth of the transition layer (of the order of a_B for our m_e/m_h ratio,[17]) $z = z_e - z_h$ is the relative *e*-*h* position in z direction, and $r = |r_e - r_h|$ is the relative electron-hole coordinate. $F_{\rm ee}$, $F_{\rm oo}$, $F_{\rm eo}$, and $F_{\rm oe}$ are general even and odd functions of z, related to the excited states of the exciton. Their analytical expression is obtained from the fulfillment of the boundary conditions and is reported in Ref. 9, while the other symbols involved in Eq. (4) have the usual meaning.

The effect of the image charge on carriers due to dielectric discontinuity at the interface is negligible in our samples, because of the reduced cadmium content in the well. For a given L_w, the effective well width $L_{\rm eff}$ increases with the quantum number n of the eigenstate, because excited states experience a smaller potential depth (a greater exciton penetration in barrier is expected with increasing n).

From the no-escape boundary conditions, we obtain the quantization of the center-of-mass wave vector K,

$$\begin{aligned}&K_n^e \tan(K_n^e L_s/2) + P\tanh(PL_s/2) = 0, \\ &\frac{\tan(K_n^o L_s/2)}{K_n^o} - \frac{\tanh(PL_s/2)}{P} = 0,\end{aligned} \tag{5}$$

for even and odd wave functions, respectively. The continuous polariton curve takes discrete values in correspondence of the K_n's given by Eqs. (5).

Starting from the variational wave functions, we compute the normal-incidence optical response of the system[9] including polariton effects (dotted curve in Fig. 2).

In the simulation of the absorption spectra, we took $\varepsilon_\infty = 8.85$, $M_{\rm exc} = 0.7402 m_0$,[4] the α_0 bulk value is obtained from the expression of the longitudinal-transverse splitting $E_{\rm LT} = 2\pi\alpha_0 E_0/\varepsilon_\infty$ (taking $E_{\rm LT}$ from Ref. 18), while for narrow wells the α_0 value accounts for the increasing of the oscillator strength with reducing well width. Furthermore, we assume that the light hole subbands do not mix with the heavy hole, due to the large strain-induced splitting of about 40 meV.[4]

The theoretical calculations reproduce nicely the energy positions of the first center-of-mass states [Fig. 2(a)]. A small inhomogeneous broadening (1 meV) has been assumed in the calculations, whereas the absorption continuum due to the motion of the exciton in the plane of the well has been neglected.

From Fig. 2(a), we see that the $n = 3$ state of the 7-nm sample is not well resolved experimentally, due to the convolution with the inhomogeneusly broadened continuum of the QW.

From the calculations we obtain $L_{\rm eff} \simeq L_w$ for thick wells (11 nm and 20 nm). This means that the exciton motion is substantially confined in the quantum well, as expected from the small barrier penetration (less than 1 nm in our samples) and the reduced coupling between center-of-mass and *e*-*h* relative motions. In the 20 nm sample we expect to recover the three-dimensional limit ($L_{\rm eff} \gg 1/P$), which allows the use of the adiabatic approximation for the exciton-polariton dispersion curve [Eq. (3)]. In this case, indeed, we obtain

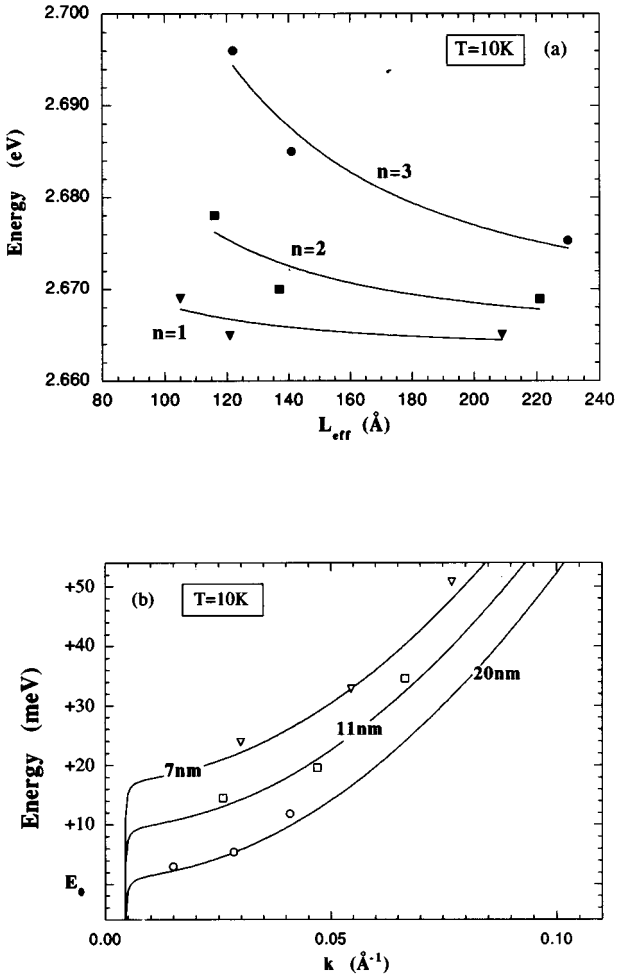

FIG. 3. (a) Well width dependence of the center-of-mass states. The symbols denote the experimental data, while continuous lines are fitting curves reproducing the $L_{\rm eff}^{-2}$ dependence of Eq. (3). (b) Experimental (symbols) and theoretical (solid lines) determinations of the lower branch of the HH exciton-polariton dispersion curve. The theoretical curves were obtained from Eq. (1), and are shown rigidly shifted upward for clarity. The value of K_n and the energy splitting is seen to increase with decreasing well width, as expected from the quantum-size dependence of the quantization conditions given in Eq. (6).

$L_{\rm eff}=209$ Å (almost equal to L_w) and $1/P=39$ Å for the $n=1$ CM eigenstate. We also note that the $n=2$ structure merges into the free-exciton peak, due to the small energy splitting between levels at this well width, thus falling into the $n=1$ free-exciton broadening. Conversely, in the 7-nm-wide well we obtain $L_{\rm eff}\simeq 1.3L_w$, evidencing relevant nonadiabatic effects of interaction between the two transition layers. Figure 3(a) displays the calculated CM eigenenergies versus the effective well width (solid lines) and the experimental positions of the $n=1$, 2, and 3 spectral features (symbols). The good agreement between theory and experiment for the eigenstates up to $n=3$ is a confirmation of the accuracy of our variational description to the exciton motion in this range of well width values. The intermediate region between the two- and three-dimensional exciton behaviors shows a clear effect of quantization of the exciton CM motion, with a smooth transition from the thin-film regime to the strong confinement regime. Indeed, the increasing deviation of $L_{\rm eff}$ from the L_w value with reduced well width demonstrates the increasing importance of the transition layer and therefore the presence of nonadiabatic effects. An additional proof that the quantization mechanism in these samples involves mainly the exciton-polariton CM motion, comes from the energy-momentum dispersion $E(k)$. In Fig. 3(b), the theoretical $E(k)$ curve obtained from Eq. (1) is plotted together with the experimental CM states (symbols), as derived from the simulations of the absorption spectra [Eqs. (5)]. The increasing separation between center-of-mass K_n values, occurring in QW's of decreasing width, reproduces the behaviour qualitatively expected from Eq. (2).

Finally, we would like to comment on the selection rules of the optical transistions involving center-of-mass states. In our intermediate range of thickness, the splitting between the quantized carrier subbands is lower than the exciton binding energy in the well, giving an exciton description via a variational envelope function which accounts for the mixing of the various center-of-mass states. This mixing results in a modification of the radiative selection rules, allowing the observation of the otherwise forbidden $n=2$ states.[10]

IV. CONCLUSIONS

We demonstrated that the quantization of the center-of-mass motion of the exciton polariton governs the intrinsic excitonic absorption in $Zn_{1-x}Cd_xSe/ZnSe$ quantum wells at the crossover between the two- and three-dimensional exciton behaviors. We used an accurate ''*thin-slab*'' exciton envelope function within a variational approach to reproduce the polariton dispersion $E(k)$ and the well width dependence of the quantized center-of-mass states. The clear observation of quantization of the center-of-mass motion of exciton-polariton in shallow $Zn_{1-x}Cd_xSe/ZnSe$ quantum wells undoubtedly indicates an important role of free excitons in determining optical absorption even in ternary alloy quantum wells. This is rather surprising due to competing localization of excitons, which tends to suppress polariton effects, but it is confirmed by the reduced Stokes shift between absorption and luminescence spectra[4] and by pump-and-probe experiments.[5]

ACKNOWLEDGMENTS

We gratefully acknowledge the expert technical help of D. Cannoletta and M. Corrado, and the collaboration of P.V. Giugno, L. Calcagnile, R. Rinaldi, and P. Prete for help in the early stage of this work. This work is supported by the Progetto NOVA-CNR.

*Present address: Centro Materiali Biofisica Medica, I-38050 Povo, Trento, Italy.

†Also at Department of Chemical Engineering and Materials Science, University of Minnesota, Minneapolis, MN 55455 and Dipartimento di Fisica, Universitá di Trieste, Trieste, Italy.

[1] M.A. Haase, J. Qiu, J.M. DePuydt, and H. Cheng, Appl. Phys. Lett. **59**, 1272 (1991).

[2] H. Jeon, J. Ding, A.V. Nurmikko, W. Xie, D.C. Grillo, M. Kobayashi, R.L. Gunshor, G.C. Hua, and N. Otsuka, Appl. Phys. Lett. **60**, 2045 (1992).

[3] J. Ding, M. Hagerott, T. Ishihara, H. Jeon, and A.V. Nurmikko, Phys. Rev. B **47**, 10 528 (1993).

[4] R. Cingolani, P. Prete, D. Greco, P.V. Giugno, M. Lomascolo, R. Rinaldi, L. Calcagnile, L. Vanzetti, L. Sorba, and A. Franciosi, Phys. Rev. B **51**, 5176 (1995).

[5] R. Cingolani, L. Calcagnile, G. Colí, D. Greco, R. Rinaldi, M. Lomascolo, M. DiDio, A. Franciosi, L. Vanzetti, G.C. LaRocca, and D. Campi, J. Opt. Soc. B **13**, 1268 (1996).

[6] A. Tredicucci, Y. Chen, F. Bassani, J. Massies, C. Deparis, and G. Neu, Phys. Rev. B **47**, 10 348 (1993).

[7] J. Kusano, Y. Segawa, M. Mihara, Y. Aoyagi, and S. Namba, Solid State Commun. **72**, 215 (1989).

[8] N. Tommasini, A. D'Andrea, R. Del Sole, H. Tuffigo-Ulmer, and R.T. Cox, Phys. Rev. B **51**, 5005 (1995).

[9] A. D'Andrea and R. Del Sole, Phys. Rev. B **41**, 1413 (1990).

[10] H. Tuffigo, R.T. Cox, N. Magnea, Y. Merle d'Aubigné, and A. Million, Phys. Rev. B **37**, 4310 (1988).

[11] H. Tuffigo, R.T. Cox, F. Dal Bo', G. Lentz, N. Magnea, H. Mariette, and C. Grattepain, Superlatt. Microstruct. **5**, 83 (1989).

[12] L_{eff} takes into account the existence of two thin regions near the interfaces where the probability of finding the exciton is very small (*transition layer*).

[13] L. Sorba, G. Bratina, A. Antonini, A. Franciosi, L. Tapfer, A. Migliorini, and P. Merli, Phys. Rev. B **46**, 6834 (1992), and references therein.

[14] G. Bratina, L. Vanzetti, R. Nicolini, L. Sorba, X. Yu, A. Franciosi, and G. Mula, Physica B **185**, 557 (1993); G. Bratina, R. Nicolini, L. Sorba, L. Vanzetti, G. Mula, X. Yu, and A. Franciosi, J. Cryst. Growth **127**, 387 (1993).

[15] J.J. Hopfield and D.G. Thomas, Phys. Rev. **132**, 563 (1963).

[16] We assume the exciton to be a harmonic oscillator (Lorentz oscillator).

[17] A. D'Andrea and R. Del Sole, Phys. Rev. B **32**, 2337 (1985).

[18] B. Sermage and G. Fishman, Phys. Rev. B **23**, 5107 (1981).